

# Artificial aging effect on precipitation and age-hardening in an Al-Zn-Mg-Cu alloy

L. Boumaza<sup>a</sup>, L. Hadjadj<sup>a</sup>, Z. Belamri<sup>a</sup>, A. Azizi<sup>a</sup>, R. Benmelit<sup>b</sup> and D. Hamana<sup>a,c</sup>

<sup>a</sup>Unité de Recherche Sciences des Matériaux et Applications, Université Frères Mentouri Constantine1, 25000, Algérie.

<sup>b</sup>Laboratoire de Microstructures et Défauts dans les Matériaux, Université Frères Mentouri Constantine1, 25000, Algérie.

<sup>c</sup>Ecole Nationale Polytechnique de Constantine, 25000, Algérie.

\*Corresponding author, email: boumazaleila@yahoo.fr

Selected paper of JSSE'18, received in final form: March 4, 2019 ; accepted date: March 23, 2019

## Abstract

In the present work, the influence of heat treatment on the mechanical properties and precipitation of the different phases in Al-Zn-Mg-Cu alloy was studied. The precipitation sequence and the mechanism of structural hardening have been followed using the differential scanning calorimetry (DSC), the microhardness measurements, the X-ray diffraction (XRD) and the scanning electron microscopy (SEM). Five calorimetric effects have been recorded and correspond to the different phases precipitating in this system of alloys and which are: the GPI zones and / or VRC (or GPII), the intermediate  $\eta'$  phase and the equilibrium  $\eta$  phase with a suspicion concerning the existence of T and S phases. Microhardness measurements of the aged state at 226 °C confirm the existence of two types of phases: the metastable  $\eta'$  phase and the equilibrium  $\eta$  phase ( $MgZn_2$ ). The appearance of the first precipitates was followed by SEM. The fine precipitates become larger (holdings at 243 and 266 °C) and the equilibrium  $\eta$  phase continues to grow inside and on the grain boundaries to become a large spherical and/or lamellar precipitate. The X-ray diffraction confirmed that only the equilibrium  $\eta$  phase was observed in this type of alloy.

**Keywords:** AlZn-Mg-Cu; mechanical properties; heat treatments; DSC; XRD and SEM.

## 1. Introduction

The based Al-Zn-Mg-Cu alloys are widely used in the aircraft industry. The mechanical strength of these alloys is increased through precipitation of a fine dispersed phase using heat treatment process called precipitation ageing. Consequently, Guinier-Preston (GP) zones, the  $\eta'$  and  $\eta$  ( $MgZn_2$ ) precipitates are the main phases present in alloys of the 7XXX series, and the  $\eta'$  phase is primarily responsible for the increased resistance [1].

The precipitation sequence in these alloys is usually the following [2].

Solid solution  $\rightarrow$  coherent GP zones  $\rightarrow$  semi-coherent  $\eta'$   $\rightarrow$  incoherent  $\eta$  ( $MgZn_2$ ).

Instead of  $\eta$  phase, GP zone and  $\eta'$  phase are proved to be responsible for the peak strength of Al-Zn-Mg-Cu alloys. The Al-Zn-Mg-Cu system was complex. It was reported that several intermetallic phases such as  $\eta$  ( $MgZn_2$ ),  $T(Al_2Mg_3Zn_3)$ ,  $S(Al_2CuMg)$ ,  $\theta(Al_2Cu)$ ,  $Al_3CuFe$ ,  $Al_3Fe_2$  and  $Mg_2Si$  can occur below the solidus [3-5]. The  $\eta$  and T phases were often presented as solid solutions with extended composition ranges containing all four elements. The second phases based on  $\eta$  ( $MgZn_2$ ),  $T(Al_2Mg_3Zn_3)$  and  $S(Al_2CuMg)$  were present in the as cast Al-Zn-Mg-Cu alloys, and the nature of these phases was reported [6]. For the alloys after aging, the investigated of the effect of

Zn/Mg ratio on the quench sensitivity of aluminum alloy 7175 thick forging by means of DSC [7]. It is unlikely that these phases or their metastable precursors, would form in Al-Zn-Mg-Cu alloy, while the temperature and ageing time are the main parameters for the variation in the final formation of precipitates.

In this paper, the thermal aging behavior of an Al-Zn-Mg-Cu alloy has been studied. The effect of temperature and aging time on the microstructure and the mechanical properties were studied; the presentation of the precipitation as a thermally activated process was also discussed.

## 2. Experimental

The alloy of study is the commercial Al-Zn-Mg-Cu alloy (nominal composition Al-8 Zn-2.54 Mg-1.45Cu (in wt. %)). This alloy underwent, after homogenization treatment and quenching in ice water, anisothermal heating at different temperatures (226 °C, 243 °C, 266 °C) for different maintain times. The analyses were carried out in a differential scanning calorimetric and completed by microhardness measurements, X-ray diffraction and the scanning electron microscope (SEM).

For calorimetric analysis, tests were performed with a SETARAM 131 DSC apparatus. The differential scanning calorimetry has been used to define the temperature

domains corresponding to microstructure changes. The Cylindrical samples of about 70 mg in mass was used. For baseline corrections, all the DSC runs were corrected by subtracting a DSC baseline obtained from a run with an empty pan. The baseline corrections were accounted for in order to free from the parasitic effects and also in perfect measuring an accurate and reliable calorimetric heat evolution and absorption of the DSC unit. In the DSC thermograms, the exothermic and endothermic reactions were plotted upward and downward respectively. The peak temperatures of all the peaks were noted. The applied thermal cycle consisted of heating from room temperature (RT) until 480°C, holding of 10 min at this temperature and finally a cooling until room temperature under air.

Vickers microhardness in different aging states was measured at RT immediately after each aging treatment. The measurements were carried out using a Zwick/Roell ZHV $\mu$  type by applying a load of 0.1 Kg for 15 seconds. prior to each HV measurement, the surfaces of the specimen was polished mechanically using emery paper and diamond paste of 1  $\mu$ m to remove the surface reactions that may occur during the heat treatment. At least ten measurements were carried out and their average was taken as the accepted value.

The XRD patterns were collected using a PANalytical Empyrean diffractometer using Cu K $\alpha$  radiation with X-ray generator power set at 1.8 kW (45 kV and 40 mA). In order to characterize the microstructure, room temperature scans were performed in the angular range of 10° to 100° with a step size of 0.02°.

SEM examinations were performed on a JEOL FEG JSM-7200F.

### 3. Results

#### 3.1. Detection of the precipitation sequence by Calorimetric study

Generally the calorimetric study can determine the kinetic parameters of precipitation and dissolution in metallic alloys like the Al-Zn-Mg-Cu alloys [8]. The DSC curve of a homogenized and quenched sample in iced water shows a thermogram consisting of five exothermic peaks and two endothermic ones (Figure.1).

- The first exothermic peak (peak 1) with a maximum situated around 72 °C most likely corresponds to the grouping of the solute leading to the formation of GPI zones or VRC that form during or after quenching.

-The second exothermic peak (peak 2) located around 160 °C is due to the formation of intermediate precipitates such as the GPII zones or the  $\eta'$  phase. The germination of  $\eta'$  may begin at about 165 °C either on GP zones [9], or by their transformation, if thereof reach a critical size [10], or directly from the VRC.

- The third exothermic peak (peak 3) at 226 °C corresponds to the formation of particles of the equilibrium  $\eta$  phase or to its different types. It is generally

believed that  $\eta$  precipitates are formed by transformation of  $\eta'$  phase and have a same hexagonal structure [11]. The fourth peak (peak 4) located around 243 °C could correspond to the formation of the T phase [10], obtained by the reduction of Zn in the solid solution (increased Mg: Zn ratio) due to the prior formation of precipitates of the  $\eta$  phase rich in Zn [12].

-The fifth peak (peak 5) at 266 °C corresponds to the formation of the S phase which was observed by transmission electron microscopy (TEM) in the form of lath-shaped lath which precipitates along the directions (001) Al in the TEM [110] Al image [10]. In addition, it has been noted the presence of  $\eta$  phase or its different variants ( $\eta_2$ ,  $\eta_4$ ) or ( $\eta_4$ - $\eta_7$ ) phases [13].

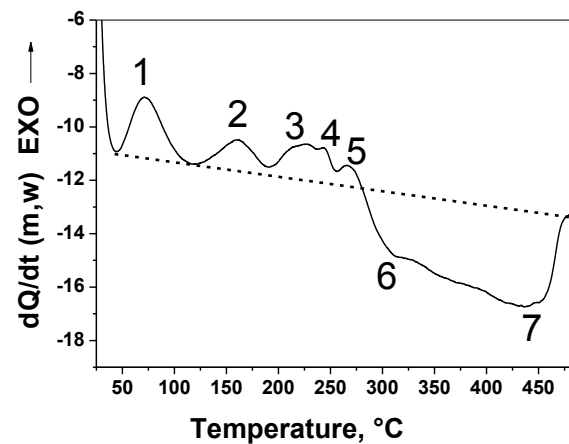


Figure 1. The DSC curve obtained at a heating rate of 10 °C/min for the quenched sample.

- At the end of curve it is noticed the presence of two endothermic peaks (peak 6 and 7), whose minimums are located at 320 °C and 437 °C, they are due to the dissolution of the previously formed phases.

#### 3.2. The artificial aging study

In order to identify the reactions that accompany the various calorimetric effects, the samples are homogenized, quenched and heated to the temperatures of the peaks 3-5 observed on the DSC curve. The samples are studied by microhardness, x-ray diffraction and SEM observations.

##### 3.2.1. Microhardness study

Figure 2 presents the microhardness curve corresponding to the last three exothermic peaks (226 °C, 243 °C and 266 °C) observed on the DSC curve.

- For the sample aging at 226 °C, it is noticed the gradual increase in microhardness values between one minute and 15 minutes, this increase starts at  $158 \pm 4.09$  N / mm<sup>2</sup> and reaches  $192.11 \pm 2.93$  N / mm<sup>2</sup>. Then a progressive decrease for holding times between 30 min and 6 hours, this decrease starts at  $154.3 \pm 2.54$  N / mm<sup>2</sup> value and ends at  $105.62 \pm 2.97$  N / mm<sup>2</sup> value. The hardness in this curve indicates the presence of two types of different phases.

The  $\eta'$  phase is formed during the heating for the first aging times where the hardness has a maximum value. The extending of the holding time leads to the transformation of this metastable  $\eta'$  phase to the equilibrium  $\eta$  phase.

- The hardness reaches a maximum value ( $173.5 \pm 2.45$  N / mm<sup>2</sup>) for a heating up to 243 °C. This value is followed by a gradual decrease in microhardness for the first holding times between 5 and 30 min and has reached  $119 \pm 2.31$  N / mm<sup>2</sup>. The increase in the holding time leads to a significant decrease which reaches  $81.16 \pm 2.48$  N / mm<sup>2</sup> for an aging of 6 hours at 243 °C. This decrease is most due to the formation of the equilibrium  $\eta$  phase.

- For the first aging times (1-5 min) at 266 °C the hardness reaches maximum values which reaches  $188 \pm 3.31$  N / mm<sup>2</sup>, then falling Hv values product and reaches  $124.71 \pm 3.63$  N / mm<sup>2</sup> for aging for 10 min. In addition, it is noted that the increase in the holding time at 266 °C leads to a rapid decrease in the values of the microhardness which reaches a minimum value of  $81.14 \pm 2.91$  N / mm<sup>2</sup> for an aging of 6 hours. As a result, this decrease is explained by the increase of the amount of the equilibrium precipitates and their growth at this temperature.

-It is noted that the microhardness curves corresponding to the temperatures 243 °C and 266 °C come together from the 60 minute maintain and are superimposed, this being explained by the fact that from 60 minutes the formation of the equilibrium precipitates is practically with the same kinetics and the same magnitude; which means that for temperatures above 243 °C the kinetics of precipitation is the same except at the first maintain times (less than 60 min) where a faster kinetics (abrupt reduction of Hv for the maintenance of 266 °C) are observed for the maintenance at 266 °C.

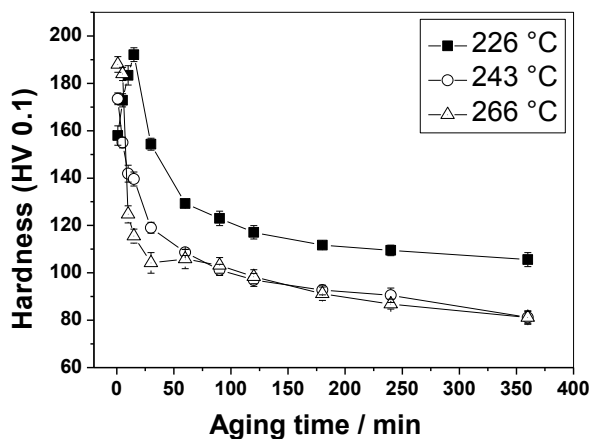


Figure 2. The evolution of microhardness as a function of aging time .

### 3. 2.2. XRD study

Figure 3 shows the X-ray diffraction spectrum of as quenched sample and then heated up to 226 °C and aged for 5min, 30min, 3h and 6h. For an aging of 5 min, the spectrum shows the peaks related to the supersaturated solid solution  $\alpha$  (Al) and two other types of intermetallic phases Mg<sub>2</sub>Si and Al<sub>2</sub>CuFe<sub>4</sub>. For an aging of 30 min, a

shoulder is noted between the two peaks 38° and 44°. This shoulder gives birth to the peaks of the equilibrium  $\eta$  (MgZn<sub>2</sub>) phase (according to ASTM card 34-0457) for an aging of 3h, as we can see the distribution of the low intensity peaks which always correspond to the same equilibrium  $\eta$  phase. The increase of the holding time up to 6h leads to a considerable increase in the intensity of the peaks of the equilibrium  $\eta$  phase. That is, the disappearance of the diffraction peaks of the equilibrium phase during the first aging time of 5 min indicates that this period is insufficient for the formation of this phase. The drop in microhardness values for aging of 30min was detected by XRD and is explained by the onset of the birth of the equilibrium  $\eta$  phase. In addition, for the aging of 3h and 6h, the majority of the diffraction peaks of the equilibrium phase appear and the increase in the intensity of these peaks indicates a good quantity of this formed equilibrium phase for an aging of 6h where the hardness decreases. The formation of  $\eta$  phase is very slowly for aging for 226 °C, it is moderately fast for the aging of 243 °C and at higher aging temperatures (266 °C) the  $\eta$  phase formed more rapidly ( $\sim 5$  min). Here, it is the only precipitated phase observed, even for an aging of 6 hours. In addition, the diffraction peaks of the intermetallic phases (Mg<sub>2</sub>Si and Al<sub>2</sub>CuFe<sub>4</sub>) are always present in the diffraction spectra, which implies that these secondary particles cannot be dissolved in the matrix after the heat treatments at the temperatures chosen in our study. For the samples heated and aged at 243 °C and 266 °C, only the equilibrium  $\eta$  phase was observed, whereas no peak associated with the T and S phases could be identified in this alloy. However, this does not mean that these phases are absent from the samples, perhaps the quantity of these precipitated phases is too small (<5 nm), and that they are very difficult to detect by powder diffraction technique.

### 3. 2. 3. SEM study

The scanning electron micrograph of a homogenized sample, quenched, heated to 226 °C and aged for 6h (Fig. 4a) shows the distribution of precipitates which are pretty thin and dense and can hardly be distinguished from each other ones. This microstructure of precipitates may be due to the distribution of the  $\eta'$  phase and/or the  $\eta$  phase in the matrix of aluminum. Moreover, it is clear to note the existence of two types of precipitation: intergranular precipitation on the grain boundaries and intragranular precipitation inside the grains. The microstructure of the homogenized sample, quenched and heated to 243 °C and then aged for 6h (Fig. 4b) is not very different from one of the previous state (aged at 226 °C). The sample aged at 266 °C (Fig. 4c) has a clearer microstructure than the preceding states, the distribution of the finely dispersed precipitates in the spherical and lamellar shape are the MgZn<sub>2</sub> precipitates. we find that the microstructure observed for the aged states at 243 °C and 266 °C are almost similar. This result is good agreement with the values of microhardness for these two temperatures (243 and 266 °C) where it was observed the same kinetics for a holding time greater than 1h.

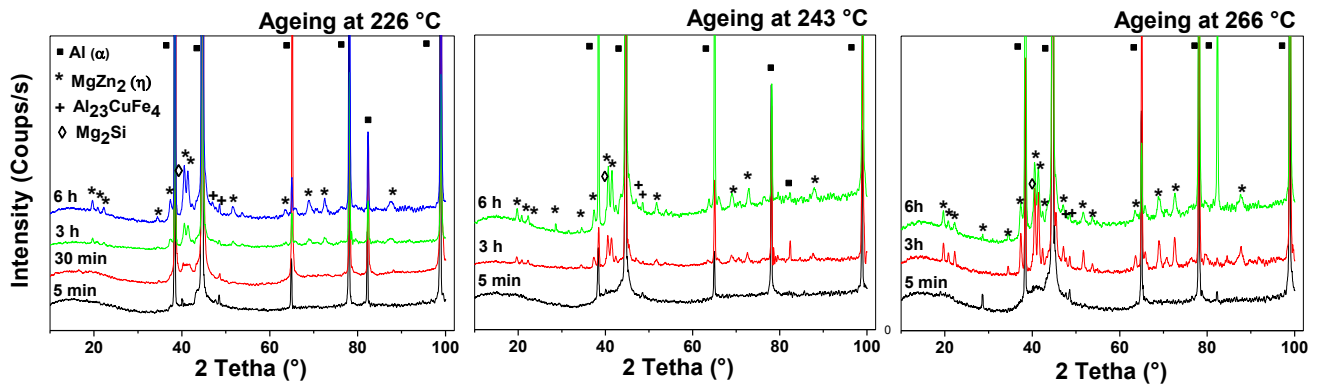


Figure 3. X-ray diffractogram of a quenched sample heated and aged at 226 °C, 243 °C and 266 °C for a different period.

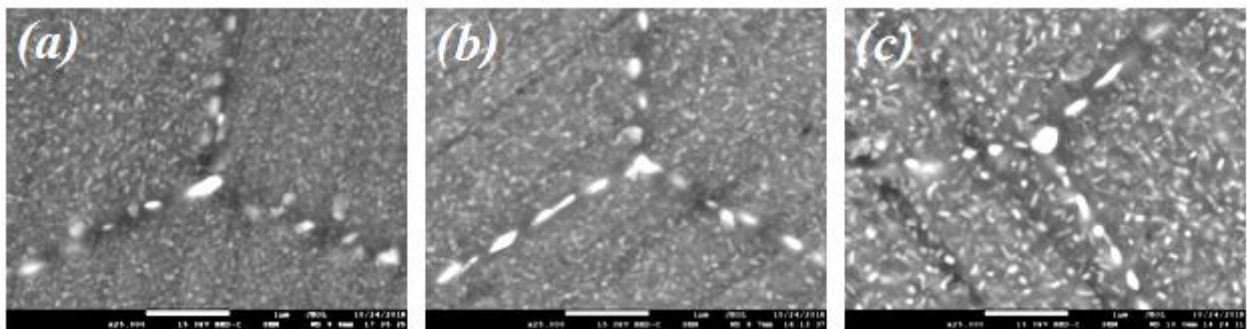


Figure 4. Typical SEM-BED images of treated samples for 6h at: (a) 226 °C, (b) 243 °C and (c) 266 °C.

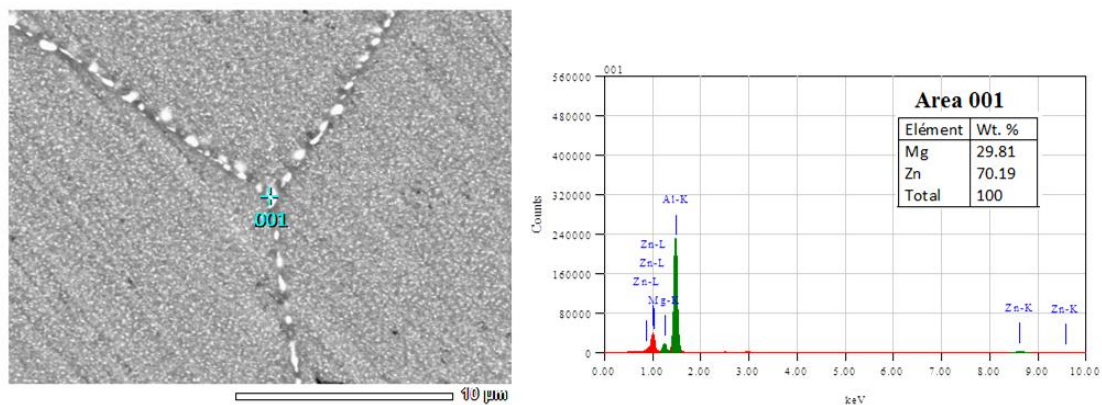


Figure 5. SEM-BED images and EDS spectrum of quenched and aged sample at 266 °C for 6h.

The nature of the precipitates were carried out using SEM, EDX analyses (Fig. 5). For the sample heated then aged for 6h at 266 °C, one can notice a white coarse precipitate on the grain boundaries. The EDX analysis of this precipitate shows the presence of Mg and Zn elements. this is the  $MgZn_2$  ( $\eta$ ) phase. where the atomic content for Zn was about twice that of Mg.

#### 4. Conclusion

The main results obtained during this work can be summarized as follows:

- Five calorimetric effects recorded during heating with a speed of 10 °C / min between 30- 480 °C, these effects correspond to the GPI zones and/or VRC and GPII zones, the intermediate  $\eta'$  phase and the equilibrium  $\eta$  ( $MgZn_2$ ) phase with a suggestion about the existence of T and S phases.
- Microhardness measurements of the aging state at 226 °C confirm the existence of two types of phases:  $\eta'$  and  $\eta$ . The extending of the aging time leads to the transformation of the metastable  $\eta'$  phase to the equilibrium  $\eta$  phase.
- The hardness value obtained during heating and ageing at 243 °C appears to be different to one of ageing at 226 °C, but this difference is not detected by XRD. The extension of the holding time always leads to the precipitation of the same equilibrium  $\eta$  phase.
- The study at 266 °C shows that the formation of equilibrium phase is very fast at this temperature. Spherical and lamellar precipitates were observed by SEM.
- X-ray diffraction makes it possible to follow the birth of the first precipitates of the  $MgZn_2$  phase and their growth by prolongation the holding time at 226 °C, 243 °C and 266 °C.

- The kinetic of precipitation is the same for the two aging temperatures at 243 °C and 266 °C for the maintain times greater than 60 min.

#### References

- [1] S. C. Jacumasso, J. de P. Martins, A. L. M. de Carvalho, International Engineering Journal, 69 (2016) 451.
- [2] V. Hansen, O B . Karlsen, Y. Langsrud, Materials Science and Technology, 20 (2004) 185.
- [3] F. Y. XIE, X. Y. Yan, L. Ding, F. Zhang, S. L. Chen, M. Chu and Y. A. Chang., Mate Sci Eng A, 335 (2003) 144.
- [4] L. L. Rokhlin, T. V. Dobatkina, N. R. Bochvar, E. V. Lysova, Journal of Alloys and Compounds, 367 (2004) 10.
- [5] X. M. Li, M. J. Starink, Mate Sci. Tech. 17 (2001) 1324.
- [6] C. Mondal, A. K. Mukhopadhyay, Materials Science and Engineering A, 391 (2005) 367.
- [7] S.T. Lim, S. J. Yun, S. W. Nam, Materials Science and Engineering A, 371 (2004) 82.
- [8] S. Ghosh, N. Gao., Rans. Nonferrous Met. Soc. China, 21 (2011) 1199.
- [9] E. Salamci, Turk Journal of Engineering and Environmental Science, 25 (2001) 681.
- [10] J. Buha, R.N. Lumley, A.G. Crosky , Materials Science and Engineering A, 492 (2008) 1.
- [11] T. Marlaud, (2008), Matériaux. Institut National Polytechnique de Grenoble - INPG, France.
- [12] J.K. Park, A.J. Ardell, Materials Science and Engineering A, 114 (1989) 197.
- [13] G. Thomas, J. Nutting, Journal of the Institute of Metals, 88 (1960) 81.